# The Role of Plant Water Storage on Water Fluxes within the Coupled Soil-Plant System

Cheng-Wei Huang \*1, Jean-Christophe Domec<sup>1,4</sup>, Eric J. Ward<sup>2,3</sup>, Tomer Duman<sup>5</sup>, Gabriele Manoli<sup>1</sup>, Anthony J. Parolari<sup>1,6</sup>, and Gabriel G. Katul<sup>1,6</sup>

<sup>1</sup>Nicholas School of the Environment, Duke University, Durham, North Carolina, USA.

<sup>2</sup>Department of Forestry and Environmental Resources, North Carolina State

University, Raleigh, North Carolina, USA.

<sup>3</sup>Ecosystem Science Group, Environmental Sciences Division, Oak Ridge National Laboratory, Oak Ridge, Tennessee, USA.

<sup>4</sup>Bordeaux Sciences Agro UMR 1391 INRA-ISPA, University of Bordeaux, Gradignan, France.

<sup>5</sup>Department of Biological Sciences, Rutgers University, Newark, New Jersey, USA. <sup>6</sup>Department of Civil and Environmental Engineering, Duke University, Durham, North Carolina, USA.

May 21, 2016

#### Word counts

Summary: 199

Main body: 6496

Introduction: 625

Description: 3068

Results: 700

Discussion: 2055

Acknowledgments: 48

Number of figures:10

Color figures:Fig.1, 3, 4, 5, 6, 8, 9, 10

Number of tables:1

**Supporting information**: 5 tables and 4 figures

<sup>\*</sup>Email: cheng.wei.huang@duke.edu Tel: +1 919 536 8252

#### Summary

- 1. In addition to buffering plants from water stress during severe droughts, plant water storage (PWS) alters many features about the spatio-temporal dynamics of water movement in the soil-plant system. How PWS impacts water dynamics and drought resilience is explored using a multi-layer porous media model.
- 2. The model numerically resolves soil-plant hydrodynamics by coupling them with leaf-level gas exchange and soil-root inter-facial layers. Novel features of the model are the considerations of a coordinated relation between stomatal aperture variation and whole-system hydraulics and the effects of PWS and nocturnal transpiration ( $F_{e,night}$ ) on hydraulic redistribution (HR) in the soil.
- 3. The model results suggest that daytime PWS usage and  $F_{e,night}$  generate residual water potential gradient  $(\Delta \psi_{p,night})$  along the plant vascular system overnight. This  $\Delta \psi_{p,night}$  represents a non-negligible competing sink strength that effectively diminish the significance of HR.
- 4. Considering the co-occurrence of PWS usage and HR during a single extended dry-down, a wide range of plant attributes and environmental/soil conditions selected to enhance or suppress plant drought resilience is discussed. When compared to HR, model predictions suggest that increased root water influx into plant conducting tissues overnight maintain a preferable water status at the leaf thereby delaying the onset of drought stress.

**Keyword**: drought resilience; hydraulic redistribution; leaf-level gas exchange; nocturnal transpiration; plant water storage; root water uptake

### 1 Introduction

23

24

25

26

27

28

29

30

31

32

33

35

36

37

38

40

41

42

43

44

The ability of xylem tissues to store water is perceived to be part of an evolutionary process that supports physiological function for the whole-plant during severe drought conditions (Tyree and Ewers, 1991; Cruiziat et al., 2002; McDowell et al., 2008; Manzoni et al., 2014; Parolari et al., 2014; Sperry and Love, 2015). However, the beneficial effects of plant water storage (PWS) on a wide range of soil-plant hydrodynamic processes has received far less attention. A 5 defining feature of PWS is a time lag between basal sap flux and crown transpiration (Phillips et al., 2004; Chuang et al., 2006). In large tree species and during severe drought conditions, empirical evidence suggests that a significant amount of whole-plant transpiration originates from PWS (Waring and Running, 1978; Waring et al., 1979; Schulze et al., 1985; Goldstein et al., 1998; Maherali and DeLucia, 2001; Phillips et al., 2003). In the presence of PWS, whole-10 plant transpiration rate exceeds basal sap flux during early morning hours signifying a discharge 11 from PWS. During late afternoon and proceeding into the evening, the basal sap flux can exceed 12 whole-plant transpiration rate suggesting partial refilling of PWS and adjusting xylem pressure 13 to less negative values. These adjustments in xylem pressure may be significant in repairing 14 embolized xylem vessels through bubble dissolution (Waring and Running, 1978; Tyree and 15 Sperry, 1989; Konrad and Roth-Nebelsick, 2003). Such modifications by PWS beg the question 16 as to how root water uptake (RWU) and hydraulic redistribution (HR) in soils as well as leaf-17 level transpiration rates are impacted by the presence of PWS. At sites where leaf-level gas 18 exchange occurs, the presence of PWS may allow leaves to maintain a water potential state 19 beneficial to carbon uptake over a longer time period (Goldstein et al., 1998; Stratton et al., 2000; 20 Maherali and DeLucia, 2001). However, a daytime dehydration of PWS may reduce beneficial 21 contributions arising from overnight HR due to a competing sink that must be recharged. 22

One recent review covering the magnitude of HR across a wide range of ecosystems and environmental conditions (Neumann and Cardon, 2012) offers a tantalizing clue that the magnitude of HR predicted by previous models that ignored PWS or nocturnal transpiration  $(F_{e,night})$  is consistently higher than those reported by empirical studies. This over-prediction of HR occurs despite model differences in the mechanics of incorporating HR (Siqueira et al., 2008) or in assumed root density profile properties (Schymanski et al., 2008). It has been foreshadowed by Neumann and Cardon (2012) that the exclusion of an above-ground competing sink strength (due to finite PWS or  $F_{e,night}$ ) in such models can be a plausible explanation for the consistent overestimation, which is another motivation for the work here.

The objective is to disentangle the effects of PWS and  $F_{e,night}$  on water fluxes from the soil to the leaf from other hydraulic traits on diurnal to daily-time scales. The approach to be followed is based on a vertically resolving numerical model for both the soil and plant systems. This model combines soil-plant hydrodynamics with leaf-level physiological and soil-root constraints. Thus, the leaf-level gas exchange can be impacted by soil water availability through the water potential gradient from the leaf to the soil, and vice versa. The focus here is on forested ecosystems where PWS may be significant during an extended dry-down period. The dry-down time scale is assumed to be sufficiently long to allow PWS to experience multiple discharge-recharge phases under different soil moisture states but sufficiently short so that hydraulic, eco-physiological, leaf area, root distribution, and concomitant allometric properties do not vary appreciably. The model results are then analyzed with particular attention to exogenous environmental factors and endogenous plant attributes promoting the use of PWS versus direct soil water through eight scenarios. While a large number of hydrological and ecological studies have already documented the benefits of HR on carbon-water relations (Domec et al., 2010; Prieto et al., 2012), conditions where plant hydraulic capacitance or  $F_{e,night}$  may compete with HR remain unclear. Hence, the overnight competition for water between above-and below-ground reservoirs is discussed through model calculations. The discussion of the model results finally focuses on the responses of leaf-level gas exchange to progressive drought conditions in the context of the functional role of PWS versus HR.

## 51 2 Description

#### 52 2.1 Modeling framework

There is a plethora of complications when modeling/measuring plant water relations in forested ecosystems including inhomogeneity in leaf arrangements, the plant and soil hydraulic properties, the rooting system, and the temporal variability in environmental variables. Moreover, plant-plant interactions such as competition for light or water and the dynamic nature of plant hydraulic and physiological properties over long time scales (e.g., seasonal) necessitate an intermediate level of modeling approaches as discussed elsewhere (Bohrer et al., 2005). In this approach, the bulk water movement along the primary pathways is modeled with much of the finer scale spatial processes (e.g., cavitation, soil-root contact) being surrogated to non-linearities in hydraulic properties. Hence, within each of the soil-plant compartments, the goal is to retain sufficient representation of key hydrodynamic and physiological processes while allowing for integration to the plant level.

Starting with the above-ground plant compartment, a logical choice is to adopt a 'macroscopic' (i.e., tissue level) approach in analogy to the soil system. The bulk effect of 'microscopic' processes (i.e., cell or pore level) are embedded in the shape of the vulnerability curve and PWS as they relate to xylem water potential. It is to be noted that xylem conduits are more elongated and their diameters are less variable when compared to soil pores. Despite this pore structure difference, the flow and energy losses to friction can still be reasonably approximated by Darcy's law. Hence, a one-dimensional porous media model is employed to describe the transient water flow from the stem base to the leaf parameterized with literature-reported hydraulic attributes of plant tissues. The soil water supply to the plant is represented using a conventional multi-layered scheme that employs Richard's equation adjusted by soil-root interactions reflecting root water influx or efflux (i.e., possible HR). These inter-facial transfer processes depend on soil-to-root conductances along the flow path and the lateral energy gradient between the soil and the root at a given depth.

The porous-media analogy representing water flow through each compartment of the soil-plant system and connections between them is capable of capturing the main features of macroscopic water flow pertinent to PWS dynamics. The complex features of plant hydraulic architecture are not explicitly resolved but the effects of tree size and vertically non-uniform root distribution on plant water relations are captured. The leaf-level water balance employed here provides a representation accounting for the nonlinear relations between stomatal aperture and the time-history of leaf water potential. The latter is limited by soil water availability and the interplay between biological controls through stomata and the aerodynamic modifications due to wind speed. This modeling approach is illustrated in Fig. 1 and detailed information of the formulations and assumptions is given next. The notation and units used throughout are listed in Supporting Information.

#### 2.2 Plant conducting tissues

Water transport through tracheid aggregates or vessels inter-connected by end-wall pits in the water conducting tissues can be treated as analogous to porous media flow (Edwards et al.,

1986; Tyree, 1988; Früh and Kurth, 1999; Kumagai, 2001; Aumann and Ford, 2002; Bohrer
et al., 2005; Chuang et al., 2006; Hentschel et al., 2013; Manzoni et al., 2013c,a, 2014). Thus,
a mass conservation equation is combined with Darcy's law to describe the water movement at
the tissue-scale and is given as

$$\frac{\partial V_s(z)\theta_p(z,t)}{\partial t} = -\frac{\partial q_p}{\partial z}dz$$

$$q_p = -A_s(z)K_p(\theta_p)\frac{\partial \psi_p}{\partial z}$$

$$\psi_p = \phi_p + \rho gz$$
(1)

where  $V_s(z) = \int_z^{z+\Delta z} A_s(z) dz$  is the sapwood volume between height z and  $z + \Delta z$  above the soil surface,  $\theta_p$  is the plant (or xylem) water content, and  $q_p(z)$  is the sap flow rate driven by gradients in total water potential,  $\psi_p$ .  $\rho$  is the water density, g is the gravitational acceleration,  $K_p$  is the plant hydraulic specific conductivity, and  $A_s(z)$  is the sapwood area profile representing the effective cross-sectional area of conducting tissues.  $\psi_p$  includes plant pressure potential (i.e., xylem matric potential),  $\phi_p$ , and the gravitational potential  $\rho gz$  but ignores the kinetic energy head and assumes negligible variations in osmotic potential for long distance water flow in the xylem (Früh and Kurth, 1999). A cone-shaped tree volume is adopted to represent the effective tree dimensions using only tree height (H) and  $A_s(z)$  that is linked to H by

$$A_s(z) = A_{s,base} \left( 1 - \frac{1}{2} \frac{z}{H} \right)^2, \tag{2}$$

where  $A_{s,base}$  is the sapwood area at stem base.

In the plant vascular system, the percentage of  $K_p$  loss referenced to the maximum specific conductivity  $K_{p,max}$  at saturation  $\theta_{p,sat}$  due to a reduced  $\phi_p$  is commonly described by the vulnerability curve:

$$K_p(z) = K_{p,max} \exp\left[-\left(\frac{-\phi_p(z)}{c_1}\right)^{c_2}\right],\tag{3}$$

where  $c_1$  and  $c_2$  are constants describing its shape. The monotonic relation between  $\theta_p$  and  $\phi_p$  is approximated by a *plant retention curve* and is given by (Chuang et al., 2006):

$$\frac{\theta_p(z)}{\theta_{p,sat}} = \left(\frac{\phi_0}{\phi_0 - \phi_p(z)}\right)^p,\tag{4}$$

where p and  $\phi_0$  are constants. This formulation ensures  $\phi_p = 0$  at saturation and represents the degree of relative change in  $\theta_p$  with respect to  $\phi_p$  through p. The plant 'retention curve' can be further used to infer the specific hydraulic capacitance of a plant tissue  $C_p = \partial \theta_p / \partial \phi_p$  by which the whole-plant hydraulic capacitance  $C_{p,total} = \int_0^H A_s C_p dz$  can be defined to describe the ability to store or extract water for a unit change in  $\phi_p$ .

Unlike soils, there are a number of potential mechanisms responsible for changes in PWS. These include elasticity, capillarity and cavitation release. They were proposed by Zimmermann (1983) and experimentally shown by Tyree and Yang (1990) to be present in woody cells (i.e., xylem conduits). Unlike living cells (e.g., phloem), woody cells have rigid walls with high elastic modulus so that the elastic storage in xylem conduits due to alternating shrinkage and swelling may be minor (Brough et al., 1986). The capillary storage, which occurs in cavitated conduits, can release water by bringing the menisci towards the narrow ends of tracheids or vessels when

water potential decreases but store water in the opposite way. This implies that cavitated conduits can still partially maintain a water continuum (Tyree and Zimmermann, 2002). Since capillary storage can rapidly release or store water, Brough et al. (1986) demonstrated that the diurnal pattern of the xylem water content can be attributed mainly to such capillarity mechanism. Under sufficiently low water potential condition, the water release through cavitation events occurs when the water-filled volume is replaced by air bubbles (Tyree and Sperry, 1989; Tyree et al., 1994). Moreover, the delay in repair of cavitated conduits can induce hysteresis in both vulnerability and plant retention curves (Sperry and Tyree, 1990; Brodribb and Cochard, 2009), which is not considered here but can be accommodated in the present framework.

The consideration of PWS adjusts  $\psi_p(z)$  along the plant vascular system and thus impacts stomatal behaviors. Stomatal closure occurs before  $\psi_p(z)$  is substantially reduced and reaches a threshold that causes 'runaway cavitation' (Bond and Kavanagh, 1999; Sparks and Black, 1999). When this threshold is reached, the more dysfunctional cells due to cavitation lead to more negative water potential and further cavitation events occur in an irreversible manner. As shown in Fig. 2a, the incipient runaway cavitation is commonly defined at  $\phi_p$  where 12 % of  $K_p$ loses occur (i.e., air-entry point;  $P_{12}$ ). The slope of the vulnerability curve reaches maximum around this threshold (Domec and Gartner, 2001). However, the onset of water stress sensed by plants (i.e., stomatal closure) is dictated by a critical xylem water potential (i.e.,  $P_c$ ) that may be larger than  $P_{12}$ . It is to be noted that  $P_c$  and the corresponding loss of  $K_p$  are not a priori specified here (see Section 2.4).

#### 2.3 Soil-root interaction

122

123

124

125

126

127

128

129

130

131

133

134

135

136

139

140

141

142

144

146

147

148

151

152

153

Water transport in unsaturated soils is described by one-dimensional Richards' equation modified 143 to include water uptake/release by the rooting system within each soil layer. Hence, at each soil layer, an 'effective' source/sink term  $Q_r$  is added (Volpe et al., 2013; Manoli et al., 2014; Bonetti et al., 2015) to yield:

$$\frac{\partial \theta_s(z_s, t)}{\partial t} = -\frac{\partial q_s}{\partial z_s} - Q_r(z_s, t)$$

$$q_s = -K_s(\theta_s) \frac{\partial \psi_s}{\partial z_s}$$

$$\psi_s = \phi_s - z_s$$
(5)

where  $\theta_s$  is the soil water content at depth  $z_s$  below the soil surface,  $q_s$  is the Darcian flux driven by the vertical gradient of total soil water potential  $\psi_s$ ,  $\phi_s$  is the soil matric potential,  $K_s$  is the soil hydraulic conductivity, and  $Q_r$  is the water uptake (denoted with superscript '+') or release (denoted with superscript '-') rate from absorbing roots. In Equation 5, the Clapp and Hornberger formulations (Clapp and Hornberger, 1978) are used to represent the soil water retention curve and soil hydraulic conductivity function, and are given by:

$$\phi_s = \phi_{s,sat} \left( \frac{\theta_s}{\theta_{s,sat}} \right)^{-b}, \tag{6}$$

$$K_s = K_{s,max} \left(\frac{\theta_s}{\theta_{s,sat}}\right)^{2b+3},\tag{7}$$

where  $\theta_{s,sat}$ ,  $\phi_{s,sat}$  and  $K_{s,max}$  are the near saturated water content, air entry water potential and saturated hydraulic conductivity, respectively, and b is an empirical constant that varies 155 with soil texture.

Contributions to soil water storage (i.e.,  $\partial \theta_s/\partial t$ ) by the flux-gradient term are often referred to as the *Darcian redistribution* (i.e.,  $-\partial q_s/\partial z_s$ ). The depletion or replenishment rate of soil water storage through  $Q_r$  is determined by the water potential gradient across the root membrane and the average path length traveled radially by water molecules from the soil to the soil-root interface in series and is given as:

$$Q_r = -k \left[ (\psi_{sb} - z_s) - \psi_s \right] a_R$$

$$k = \frac{k_r k_s}{k_r + k_s}$$
(8)

where k is the total soil-to-root conductance,  $\psi_{sb}$  is the water potential at the stem base,  $a_R =$  $2\pi rB$  is the root surface density, r is the effective root radius, B is the root length density,  $k_r$ and  $k_s = K_s/l$  are respectively the root membrane permeability and the conductance associated with the radial flow within the soil to the nearest rootlet, and  $l = 0.53/\sqrt{\pi B}$  is the length scale characterizing the mean radial distance for the movement of water molecules from the bulk soil to the root surface within the rhizosphere (Vogel et al., 2013). Formulated in this manner, the root water potential  $\psi_r$  is hydrostatically distributed (i.e.,  $\psi_r = \psi_{sb} - z_s$ ) assuming that the water storage and energy losses are negligible within the transporting roots (Lafolie et al., 1991; Siqueira et al., 2008). When compared to above-ground compartments, significantly larger hydraulic conductivity (Kavanagh et al., 1999) but smaller water storage capacity (Waring et al., 1979) in the rooting system suggests that this assumption may not be too restrictive for tree species. Independent model runs also confirm the negligible effects of root water storage and resistance on both above- and below-ground water dynamics so that they are not considered hereafter. The coupling between the below- and above-ground plant system is accomplished by imposing a continuous water potential from soil  $(\psi_s)$  to stem base  $(\psi_{sb})$  and its resulting 'net' root water uptake  $(RWU_{net})$  supplied to the stem base can be expressed by the water balance for the bulk rooting system:

$$q_{p,sb} = RWU_{net} = \left[ \int_0^{L_R} (Q_r^+ + Q_r^-) dz_s \right] \rho A_{soil}$$
 (9)

where  $q_{p,sb}$  is the sap flow rate at the stem base,  $A_{soil}$  is the soil surface area covering the roots, and  $L_R$  is the rooting depth.

During daytime, inevitable water loss from leaves creates a significant water potential gradient from roots to leaves and induces water extraction throughout the rooting system (i.e.,  $Q_{r,day}^- = 0$  for all  $z_s$ ) if the upper layers of the soil are not too dry and do not serve as competing sinks. However, the root water uptake at night from wet soil layers may be released back to dry soil layers or refills the xylem volume where the xylem water has been depleted by previous daytime transpiration. While the former mechanism is commonly coined as 'hydraulic redistribution' and the amount of redistributed soil water through the rooting system can be quantified by  $\left| \int_0^{L_R} Q_r^- dz_s \right| \rho A_{soil}$ , the 'nocturnal refilling' to PWS is used to emphasize the later mechanism.

#### 2.4 Leaf-level water balance

The water balance in the foliage described elsewhere (Kumagai, 2001) is modified to include a leaf-lamina resistance and is used as the upper boundary condition for water transport within

the plant system. The leaf-level water balance can be given as:

$$A_{l}(\Delta z_{l}) \left[ C_{l} \frac{\partial \psi_{l}}{\partial t} \right] = -\left[ q_{p,top} - F_{e} \right]$$

$$q_{p,top} = A_{l} \frac{(\psi_{p,top} - \psi_{l})}{r_{l}}$$

$$(10)$$

$$F_e = A_l f_e m_v$$

where  $A_l$  is the leaf area,  $\Delta z_l$  is the effective leaf thickness,  $\psi_l$  is the leaf water potential,  $C_l$  is the hydraulic capacitance of the leaf,  $r_l$  is the leaf-lamina resistance,  $q_{p,top}$  is the sap flux entering the leaf,  $F_e$  is the total crown transpiration flux,  $\psi_{p,top}$  is the water potential at the distal conductive segment attached to the leaf, and  $f_e$  is the leaf-level transpiration rate that can be converted to mass-based units using the molecular weight of water  $m_v$  and up-scaled to  $F_e$  using leaf area  $A_l$ . For simplicity,  $C_l$  is assumed to be independent of  $\psi_l$  though this dependency can be readily incorporated if known.

The consideration of the resistance to water flow through the leaf lamina is necessary because  $r_l$  may significantly contribute to whole-plant resistance that determines the leaf-level water status (Cruiziat et al., 2002; Taneda and Tateno, 2011) and in turn limits the response of the leaf-level gas exchange to drought stress. The effects of boundary layer conductance on leaf-level gas exchange is also included (Huang et al., 2015) so as to eliminate the use of vapor pressure deficit as surrogate for actual evaporative demand (i.e., well-coupled leaf-to-atmosphere condition). It is to be noted that the well-coupled condition, which is widely used to interpret responses of stomata to their environment, may not be valid in natural settings (e.g., low wind speed or prevalence of broadleaf species). Since  $F_{e,night}$  typically accounts for 10-30% of daily transpiration (Dawson et al., 2007; Caird et al., 2007; Novick et al., 2009), this water leakage from both guard cells and cuticle is also accounted for through a residual conductance  $(g_{res})$ when nighttime evaporative demand is finite. The leaf-gas exchange model utilizes a Fickian mass transfer formulation across the laminar boundary layer attached to the leaf surface, which is then combined with the biochemical demand for CO<sub>2</sub> described by the Farquhar photosynthesis model for C<sub>3</sub> species (Farquhar et al., 1980). A leaf-level energy balance (Campbell and Norman, 1998) model and an optimal water use strategy (i.e., maximizing the 'net' carbon gain at a given  $f_e$ ) are used to determine variations in stomatal conductance  $(g_{s,CO_2})$  and leaf-level assimilation rate  $(f_c)$  and  $f_e$ . The model description can be found elsewhere (Huang et al., 2015) and is not

Adopting an optimality hypothesis in the leaf-gas exchange model is equivalent to maximizing the objective function (or Hamiltonian)

$$h_a(g_{s,CO_2}) = f_c - \lambda f_e, \tag{11}$$

where the species-specific cost of water parameter  $\lambda$  is known as the marginal water use efficiency (WUE) and measures the cost of water loss in carbon units. Mathematically,  $\lambda$  is the Lagrange multiplier for the unconstrained optimization problem and is approximately constant on time scales comparable to stomatal aperture fluctuations (Cowan and Farquhar, 1977). However,  $\lambda$  can gradually increase on a daily time scale due to reduction in soil water availability during a dry-down (Manzoni et al., 2013b) and ultimately results in complete stomatal closure. The linkage between  $\lambda$  and  $\psi_l$  derived from a meta-analysis of approximately 50 species (Manzoni et al., 2011) is adopted for the description of the increasing  $\lambda$  as drought progresses and is given by:

$$\lambda(\overline{\psi}_l) = \lambda^* \frac{c_a}{c_a^*} \exp\left[-\beta \overline{\psi}_l\right] \tag{12}$$

where  $\lambda^*$  is the marginal WUE under well-watered soil conditions at a reference atmospheric  $CO_2$  concentration  $c_a^* = 400$  ppm,  $\overline{\psi}_l$  is computed as an averaged  $\psi_l$  over the previous 24 hours period and represents a hydraulic signal that constrains the variation of stomatal aperture, and  $\beta$  is a species-specific sensitivity parameter. Again, it should be emphasized that the hydraulic signal at the leaf-level,  $\psi_l$  is not an instantaneous  $\psi_l$  because the unconstrained optimization problem requires  $\lambda$  to vary on much longer time scales than fluctuations in stomatal aperture as earlier noted. Because of this time integration of  $\psi_l$ , a dynamic PWS also impacts  $g_{s,CO_2}$ , suggesting that a reduced soil water availability does not guarantee an immediate drop in  $\psi_l$ . In lieu of Ball-Berry (Ball et al., 1987) or Leuning (Leuning, 1995) semi-empirical models, the use of such optimality hypothesis to maximize  $h_a$  reflects how the regulation of water loss through stomatal guard cells respond to water status at the leaf without invoking ad hoc correction functions (e.g., Tuzet et al. (2003)) to 'externally' reduce maximum  $g_{s,CO_2}$  or  $f_e$  as deviations from well-watered soil conditions during dry-down. It also allows a direct coupling between the carbon and water economy of the leaf through  $h_a$  that must be positive to ensure optimality. To illustrate, the value of  $\lambda$  increases with decreasing  $\psi_l$  leading to a gradual stomatal closure during a dry-down until a critical point (i.e.,  $\psi_{l,c}$ ) is reached as shown in Fig. 2b. Upon assuming that stomata per se operate only with a finite optimal 'net' carbon gain (i.e.,  $h_a > 0$  when  $\lambda < \lambda_c$ ), the critical point can now be defined as  $\lambda_c$  where the carbon gain is completely canceled out by the water cost in carbon units (Fig. 2c). This assumption may be plausible and ensures no more water loss (i.e., complete stomatal closure) when finite net carbon gain (i.e.,  $h_a > 0$ ) cannot be attained by  $g_{s,CO_2}$  (inset in Fig. 2c). The duration  $(T_c)$  before complete stomatal closure is reached can then be tracked. Also, the total carbon uptake  $(C_{uptake})$  that occurs while maintaining finite assimilation is given as:

$$C_{uptake} = \int_{0}^{T_c} f_c(g_{s,CO_2}(t))dt.$$
 (13)

Thus, the species-specific  $\lambda - \overline{\psi}_l$  relation can accommodates a wide range of plant water use strategy such as isohydric/anisohydric and is hereafter referred to as a 'leaf-level hydraulic signal curve'. Furthermore, the xylem water potential with respect to  $\overline{\psi}_{l,c}$  (i.e.,  $P_c$ ) is shown to be larger than  $P_{12}$  indicating that complete stomatal closure actually occurs before runaway cavitation as discussed earlier (Fig. 2a). Hence, a coordination between stomatal closure and  $P_c$  arises naturally from the Hamiltonian to be maximized, which is one of the main novelties linking leaf-to-xylem.

#### 2.5 Model setup

231

232

233

234

235

236

237

238

239

240

241

242

244

245

246

247

249

250

251

252

253

254

255

256

258

259

260

261

262

263

264

265

267

268

269

270

272

273

Eight scenarios (S1 $\sim$ S8) were constructed to explore the variations in environmental factors and plant traits (Table 1). To contrast the effects of plant attributes on the use of PWS, HR and  $C_{uptake}$  within  $T_c$ , the parameters  $C_p$ ,  $g_{res}$ , LAI and H are reduced in scenarios S2, S3, S7 and S8, relative to S1 while all other model parameters and environmental conditions are maintained the same. Using identical total root density and  $L_R$ , the effects of root distribution are explored by a comparison between constant and power-law rooting profiles in S4 and S6, respectively. How site factors impact soil-plant water dynamics, different soil types (i.e., sandy clay loam; S4) and lower boundary conditions (i.e., constant water table; S5) are specified and compared with the S1 (sandy soil with free drainage at the bottom of the soil column). The modeling approach is designed for a single tree but can be used for whole stand/canopy when horizontal homogeneity is assumed for all soil-plant attributes across each compartment. While tree age can be accommodated by prescribed physiological, hydraulic and allometric attributes, the plant water use strategy (i.e., isohydric or anisohydric) is not assumed and is embedded in

the leaf-level hydraulic signal curve. Since the physiological, hydraulic and allometric attributes for each compartment are rarely available from a single experiment, a literature survey was conducted with a focus on coniferous species in general and pine plantation trees in specific to obtain consistent parameters (Supporting Information). For all runs, the initial conditions are specified as near saturation in the plant vascular system and the soil column across all layers. The whole system is then allowed to drain for 12 hours (i.e., one night duration) only by gravitational forces without activating leaf-level gas exchange and  $F_{e,night}$ . With this initialization, the amount of water in the system is approximately identical for all scenarios except for the cases of constant groundwater level (i.e., S5). Subsequently, the model calculations repeat with prescribed atmospheric variables on a periodic 24-hour basis (Supporting Information) and that cause leaf-level gas exchange to operate. An additional data set described in Supporting Information is specifically used to evaluate the model performance for the water usage in the plant and the soil.

#### 288 3 Results

275

276

277

278

279

280

281

282

283

284

285

286

289

290

291

292

293

294

295

296

297

299

300

301

302

303

304

305

306

307

308

310

311

312

313

314

315

316

317

#### 3.1 General features of the modeled PWS usage

Using S1 as an example, Fig. 3a shows the typical diurnal pattern of  $F_e$  and  $q_{p,sb}$  along with modeled time delay between their peaks due to PWS. The computed delay is approximately 1.5 hours and is well within the range of 0.1 to 2.5 hours reported elsewhere (Goldstein et al., 1998; Phillips et al., 2003; Bohrer et al., 2005). The daily PWS consumed can be computed by integrating the differences between  $F_e$  and  $q_{p,sb}$  when  $F_e > q_{p,sb}$ . Fig. 3b shows a larger diurnal variation in predicted  $\theta_p$  near the tree crown suggesting that the use of PWS can be primarily attributed to water depletion from xylem tissues closer to the transpiring sites. In situ experiments (Schulze et al., 1985; Loustau et al., 1996) on coniferous species also reported a pattern consistent with the modeled results here. Since the sap flow velocity within tree species is low (Granier, 1987; Dye et al., 1996; Zang et al., 1996), this finding may not be surprising especially when the water stored in the upper part of the plant can be immediately accessible for crown transpiration. The modeled daily PWS usage normalized by daily  $F_e$  and the modeled 'actual' PWS usage without normalizing are presented in Fig. 4a,b, respectively. When soil water status cannot be recovered (i.e., continued loss of soil water through transpiration and drainage) during the dry-down, the increasing reliance on PWS with respect to  $F_e$  is inevitable. This finding appears consistent with sap flow measurements reported elsewhere (Loustau et al., 1996; Phillips et al., 2003). When the soil water availability is not limited due to the presence of a shallow groundwater table (i.e., S5), the depleted water by  $F_e$  in the soil column and plant xylem tissues can be completely recovered to its previous state within a single diurnal cycle. This explains why the use of PWS as well as HR (shown later) for S5 remains constant during the dry-down. The modeled average daily PWS usage across all scenarios ranges from 1.1 to 23.3 % when normalized by daily  $F_e$  and from 0.07 to 1.61 kg m<sup>-2</sup> (ground) day<sup>-1</sup> without normalization.

#### 3.2 General features of the modeled HR

The modeled diurnal variations in  $\theta_s$  and  $Q_r$  profiles across  $L_R$  are respectively shown in Fig. 5a,b for S6, the largest HR across all eight scenarios. Although the overall  $\theta_s$  decreases with progressively drying soil conditions, HR can partially refill  $\theta_s$  in the upper layers when a finite  $\psi_s$  gradient across  $L_R$  is maintained and  $F_e$  recedes to minimum at night. In the presence of PWS and  $F_{e,night}$ , daily HR can be computed using the total  $Q_r^-$  across each layer on a daily

basis. For all runs, modeled daily HR normalized by daily  $F_e$  and modeled daily HR without normalization are shown in Fig. 6a.b, respectively. With the exception of S5, a bell-shaped HR cycle during the dry-down process emerges and reaches a maximum value when largest  $\psi_s$ vertical gradient across  $L_R$  occurs. In the early phases of the dry-down,  $\theta_s$  and  $\psi_s$  in the upper soil layers are reduced rapidly when compared to  $\theta_s$  in the deeper layers thereby generating a continuously increasing  $\psi_s$  gradient across  $L_R$  resulting in an increasing HR. After  $\psi_s$  gradient reaches a maximum across  $L_R$ , the water located within the upper soil layers become difficult to extract by roots and most of the contribution from  $Q_r^+$  to  $F_e$  is shifted to deeper soil layers. As a result, the  $\psi_s$  gradient is gradually 'evened out' resulting in a decreasing trend in HR. This dynamic drying process across the soil layers explains the bell-shaped HR cycle reported in the literature (Meinzer et al., 2004; Warren et al., 2005; Scholz et al., 2008; Prieto et al., 2010). The modeled average and maximum magnitudes of HR across all scenarios are respectively in the range of 6.3 to 16.7 % and 0.63 to 22.9 % when normalized by daily  $F_e$ , and in the range of 0.43 to 1.08 kg m<sup>-2</sup> day<sup>-1</sup> and 0.47 to 1.56 kg m<sup>-2</sup> day<sup>-1</sup> without normalization, a result more comparable to previous empirical estimates of HR (e.g., 20 % of  $F_e$  and 0.42 kg m<sup>-2</sup> day<sup>-1</sup> on average with maximum of  $1.1 \text{ kg m}^{-2} \text{ day}^{-1}$  for loblolly pine) summarized elsewhere (Neumann and Cardon, 2012). While previous modeling studies tended to provide higher HR estimates (Neumann and Cardon, 2012), the proposed approach here ameliorates such high modeled HR by accounting for the possible use of PWS and  $F_{e,night}$  (i.e.,  $g_{res}$ ) that increase residual water potential gradient at night  $(\Delta \psi_{p,night})$  and reduce the magnitude of HR.

#### 4 Discussion

320

321

322

323

324

325

326

327

328

329

330

332

333

334

335

337

338

339

340

342

343

344

345

346

347

349

350

351

352

354

355

356

357

358

359

360

361

362

363

#### 4.1 Model analysis for PWS usage

The modeled results here indicate that the use of PWS tends to diminish under two conditions: a smaller  $C_{p,total}$  by reducing  $C_p$  or H and a smaller  $F_e$  due to a reduced  $g_{res}$  or LAI. PWS usage is interpreted as the ensemble effect of water flux gradient along the transpiration stream from stem base to leaf lamina. Hence, reductions in  $F_e$  with a smaller  $g_{res}$  or LAI (i.e., S3 and S7) promotes a smaller water flux gradient that then suppresses the use of PWS. Both daytime  $F_e$  and  $F_{e,night}$  are reduced by a smaller  $g_{res}$ . It can be expected that a smaller  $C_p$  or H (i.e., S2 and S8) provides less 'available' stored water for  $F_e$  given that  $C_{p,total}$  represents an effective measure of whole-plant water storage. Since the contribution of PWS to  $F_e$  is reduced by a smaller  $C_{p,total}$ , the water flux gradient is further reduced resulting in a smaller use of PWS for S2 and S8. The increasing trend in the use of PWS with increasing tree size appears consistent with field experiments conducted for different tree sizes across different species or within the same species (Goldstein et al., 1998; Phillips et al., 2003). Unlike above-ground plant attributes, the vertical heterogeneity in root distributions may exert only minor impact on the use of PWS but potentially significant impact on  $RWU_{net}$  and  $F_e$ . The comparison for different root distributions (i.e., S4 and S6) suggest that less PWS is used for the case of a power-law root distribution (i.e., S6). Hence,  $RWU_{net}$  (i.e.,  $q_{p,sb}$ ) is reduced if the majority of root density is concentrated within the upper dry soil layers. Due to the reduction in  $RWU_{net}$ , daytime  $F_e$  appears to decrease as well. As a result, the more rapid reduction in daytime  $F_e$  when compared to  $RWU_{net}$  can be used to explain the smaller use in PWS in S6 when compare to S4. Taken together, a larger use of PWS implies a more efficient  $RWU_{net}$  to mitigate against drought conditions (i.e., maintain highest leaf photosynthesis at a given  $f_e$ ), especially when roots are competing with drainage losses (shown later). The modeled results also indicate that more PWS usage occurs in less sandy soils (i.e., S4) or shallower groundwater level (i.e., S5). In contrast to the sandier soil type, higher soil water availability conditions can be maintained

in finer-textured soil (i.e., less conductive) even though drainage is allowed. It is for this reason that the more rapid increase in  $F_e$  than  $RWU_{net}$  generates a larger PWS usage for S4. When a shallow groundwater table is imposed on the soil system, the diurnal recovery of soil water status through HR or Darcian redistribution explains why the use of PWS for S5 can be maintained constant.

#### 4.2 Model analysis for HR

366

367

368

369

370

371

372

374

375

376

377

378

380

381

382

383

384

386

387

388

389

390

391

392

393

394

395

396

397

398

399

400

401

402

403

404

405

407

408

409

410

In Fig. 7, the partitioning between nighttime HR and  $RWU_{net}$  (i.e., nocturnal refilling) normalized by total root water influx at night over the dry-down period shows how increases in nocturnal refilling suppress HR across all scenarios. Unlike the use of PWS, HR is impacted by  $C_{p,total}$  and  $F_e$  in opposite ways. The above-ground sink strength can be reduced by a smaller  $C_{p,total}$  (i.e., S2 and S8) or  $F_e$  (i.e., S3 and S7) that potentially enhance HR differently as drought progresses. When compared to S1, the  $\psi_s$  gradient driving HR for S2 and S8 is approximately the same, given a similar daytime  $F_e$  for these three scenarios. However, the  $\psi_s$  gradient for S1 is compensated for by a larger above-ground competing sink strength that directly suppresses HR. It can be stated that the soil water drawn by the rooting system at night in S1 contributes more to recharging  $\theta_p$  depleted by previous daytime  $F_e$  but not  $\theta_s$  in the drier and shallower soil layers. When  $\Delta \psi_{p,night}$  induced by  $F_{e,night}$  is ruled out, a pattern similar to what has been reported elsewhere (Hultine et al., 2003) emerges. Although the above-ground competing sink strength for S3 and S7 is smaller than S1, their  $\psi_s$  gradients driving HR cannot rapidly develop due to a reduced daytime  $F_e$  but can be retained with a longer duration when compare to S1. It is for this reason that a wider but shallower bell-shaped HR cycle is formed for cases S3 and S7, implying a larger amount of HR in total but smaller intensity of HR during the dry-down process. If nighttime evaporative demand (averaged overnight vapor pressure deficit is 0.07 kPa computed from the atmospheric forcing shown in Supporting Information; not  $g_{res}$ ) is set to zero to suppress only  $F_{e,night}$ , an immediate increase in the intensity of HR is predicted (not shown here) consistent with a number of experiments manipulating  $F_{e,night}$  (Hultine et al., 2003; Scholz et al., 2008; Howard et al., 2009; Prieto et al., 2010). Over a dry-down, the increase in modeled HR with zero  $F_{e,night}$  is approximately 10% across all scenarios. However, the model calculations suggest that the reduction in HR due to the presence of  $F_{e,night}$  may be less significant when compared to larger  $C_{p,total}$  (i.e., more than 22% reduction in HR). Among the many plant attributes affecting HR, the variation in root distribution can directly alter the pattern of  $\psi_s$  gradient along  $L_R$  even when the above-ground competing sink strength is maintained the same. If the root density is concentrated in the upper soil layers as reflected by S6 especially for coniferous species (Jackson et al., 1996; Finér et al., 1997; Andersson, 2005), significant daytime depletion of soil water in the upper layers (Fig. 5) produces a much larger  $\psi_s$  gradient that increases the magnitude of HR. A larger HR corresponding to a vertically asymmetric root distribution has been reported by other experiments and model calculations (Hultine et al., 2003; Scholz et al., 2008; Siqueira et al., 2008; Volpe et al., 2013) lending some support to the model results here.

Regarding soil texture, the comparison between S1 and S4 suggests that sandy soils result in smaller intensity and duration (i.e., frequency) of HR (Yoder and Nowak, 1999; Wang et al., 2009) when compared to their clay counterpart. Rapid drainage in coarse-textured soils impedes the development of  $\psi_s$  gradient required for the onset of HR (Burgess et al., 2000; Scholz et al., 2008). Moreover, the loss of soil-root contact (i.e., a larger l is expected here) at low  $\theta_s$  can further diminish the ability to exude water by roots (i.e.,  $Q_r^-$ ) even when the  $\psi_s$  gradient is well developed (Wang et al., 2009). Since l is held constant here with a pre-specified B for any  $\theta_s$  condition, this reduction in  $Q_r^-$  is only possible through reductions in  $K_s$  and k (see Equation 8).

As discussed earlier, HR at night can be maintained constant for the case of groundwater level adjacent to  $L_R$  (i.e., S5) given a constant  $\psi_s$  gradient generated by daytime  $F_e$ . It also implies that the magnitude of HR with a shallow groundwater level mainly depends on the magnitude of the previous daytime  $F_e$  when below-ground conditions (i.e., soil type, groundwater level and root attributes) are not appreciably varying. However, the  $\psi_s$  gradient driving HR in this case does not accumulate with progressively drying soil condition resulting in a smaller HR magnitude.

Interestingly, when combining all the factors that potentially impact the magnitude of HR, plausible explanations can be given for two conflicting empirical studies on HR with rooting system near or in contact with a groundwater table: sugar maple (Acer saccharum) with significant HR (Dawson, 1993; Emerman and Dawson, 1996) and three desert phreatophytic plants with insignificant HR (Hultine et al., 2003). Although  $F_{e,night}$  for sugar maple is among the largest reported from a literature survey (Dawson et al., 2007), the  $\psi_s$  gradient along  $L_R$  is not reduced by  $\Delta \psi_{p,night}$  when deeper roots are in contact with groundwater. Thus, the significant  $\psi_s$  gradient across  $L_R$ , which was developed by a large daytime  $F_e$  (Dawson et al., 2007), fine-textured soil type (i.e., silt loam) and asymmetric root distribution, can intensify the magnitude of HR in this case. However, the  $\psi_s$  gradient for the three desert phreatophytes may be lacking due to the combined effects of sandy soil (up to 84% sand) and small daytime  $F_e$  thereby suppressing the occurrence of HR.

#### 4.3 Combined effects of PWS and HR on the plant drought resilience

It can be conjectured that a larger  $T_c$  improves the capabilities of a plant to resist drought stress and enhance  $C_{uptake}$  over a longer period.  $T_c$  varies with different scenarios because the temporal variation in  $\overline{\psi}_l$  dictating  $T_c$  is impacted by the combined effects of  $F_e$  and  $RWU_{net}$  as well as PWS and HR. Thus, how  $RWU_{net}$  is impacted for different scenarios can be used to explore variations in  $T_c$  and  $C_{uptake}$  in relation to PWS and HR. The modeled  $C_{uptake}$  shown in Fig. 8a features an increasing trend with respect to  $T_c$  when leaf-level physiological parameters remain the same across the eight scenarios. It is suggested that  $T_c$  during a dry-down period can be used as a direct indicator to examine the extended use of soil water to sustain  $C_{uptake}$  for each of the eight scenarios. The coordinated relation between stomatal behavior and plant hydraulics in response to soil-drying is also illustrated in Fig. 9 - showing the modeled time-course of  $g_{s,CO_2}$  and water potential in each compartment as well as the corresponding  $\overline{\psi}_l$ . The  $g_{s,CO_2}$  decreases with decreasing  $\overline{\psi}_l$  (not bulk  $\psi_s$ ) because the cost of water in carbon units (i.e.,  $\lambda$ ) increases as specified by the hydraulic signal curve. Moreover, the more rapid reduction in  $\psi_s$  when compared to the smoothly varying  $\overline{\psi}_l$  indicates how PWS impacts this hydraulic signal and subsequent response of leaf-level gas exchange to drought condition.

Fig. 8b shows that the daily  $RWU_{net}$  decreases with decreasing bulk  $\theta_s$  except for S5. A shallow groundwater level can support a constant daily  $RWU_{net}$  and  $F_e$  preventing  $\overline{\psi}_l$  from being reduced to  $\overline{\psi}_{l,c}$ . This explains why  $T_c$  is indefinite unless this ideal balance between demand and supply is discontinued. To contrast the effects of atmospheric demand (i.e.,  $F_e$ ) on  $T_c$  when  $C_{p,total}$  remains the same, a larger  $T_c$  is predicted by the reduction in  $F_e$  with a reduced  $g_{res}$  (i.e., S3) or LAI (i.e., S7) in comparison to S1. Apparently,  $RWU_{net}$  needed for  $F_e$  in such cases is reduced, suggesting that a wetter soil condition and a larger  $\overline{\psi}_l$  can be maintained for a longer period to support leaf-level gas exchange. When  $C_{p,total}$  is reduced by using a smaller  $C_p$  (i.e., S2) or H (i.e., S8) compared to S1, a rapid reduction in  $\overline{\psi}_l$  was found to diminish  $T_c$  for both cases. Although the total HR and  $RWU_{net}$  in these two cases are larger than S1,  $\psi_s$  still cannot be maintained in a wetter condition when a larger amount of  $RWU_{net}$  is required due to a lack of available PWS. Adopting the two-end member for total hydraulic capacitance (i.e., S1 and

S8) as examples (Fig. 9), larger PWS to compensate for the decline in bulk  $\theta_s$  and  $\psi_l$  enhances  $T_c$  (and  $C_{uptake}$ ) as drought progresses thereby delaying the incipient reduction in  $\overline{\psi}_l$ .

Examining the model results for S4 and S6, it is evident that the magnitude of  $RWU_{net}$  is suppressed by the case of root density concentrated in the upper soil layers (i.e., S6). Unlike previous  $C_{p,total}$  comparisons,  $\overline{\psi}_l$  can be less negative (i.e., larger  $T_c$ ) due to a larger  $RWU_{net}$  provided  $C_{p,total}$  for the two cases differing in root distributions is the same. Again, a larger HR promoted by asymmetric root distribution overnight cannot directly contribute to  $RWU_{net}$  mainly occurring during daytime. Regarding soil texture, more  $RWU_{net}$  can be supported by less sandier soil (i.e., S4). Similar to the comparison for the two-end members of root distribution,  $T_c$  is increased by a larger  $RWU_{net}$  if  $C_{p,total}$  is held constant. Hence, the finer-textured soil type can prevent a rapid decline in  $\overline{\psi}_l$  and yield larger  $T_c$ .

To sum up, routing available soil water into PWS instead of HR can be more advantageous as a strategy when drought progresses and soil water availability is the main limiting factor (even in the absence of competing species). However, the significance of HR associated with enhancement of nutrient uptake through maintaining soil-root contact, rendering water to neighboring species and maintaining microbial activities cannot be overlooked (Prieto et al., 2012). Other environmental factors and plant traits can also exert positive or negative effects on  $T_c$  depending on the duration that can sustain higher  $\psi_l$  as drought progresses. Fig. 10 summarizes the conditions promoting enhancement or suppression of modeled  $T_c$  as well as HR. Despite all the simplification made in the proposed modeling approach, the framework here can serve as a 'hypothesis generator' to assess how exogenous environmental conditions and endogenous soil-root-stem-leaf hydraulic and eco-physiological properties shape plant responses to droughts. Testing such hypothesis requires coordinated field and laboratory experiments that measure water movement in all compartments of the soil-plant system.

# 483 Acknowledgments

Supports from the National Science Foundation (NSF-CBET-103347 and NSF-EAR-1344703), the U.S. Department of Energy (DOE) through the Office of Biological and Environmental Research (BER) Terrestrial Carbon Processes (TCP) program (DE-SC0006967 and DE-SC0011461), and the Nicholas School of the Environment at Duke University Seed Grant Initiative are all acknowledged.

# 489 Author Contribution

- 490 Cheng-Wei Huang, Gabriel G. Katul and Jean-Christophe Domec developed the model. Cheng-
- Wei Huang and Gabriel G. Katul wrote the manuscript. Tomer Duman, Gabriele Manoli and
- 492 Anthony J. Parolari analyzed the model results. Eric J. Ward provided sap flux data for model
- 493 evaluation.

Table 1: Eight scenarios (S1-S8) set up to explore the use of plant water storage (PWS)

	S1	S2	S3	S4	S5	S6	S7	S8
H (m)	20	20	20	20	20	20	20	10
$C_p \; (\mathrm{kg} \; \mathrm{m}^{-3} \; \mathrm{MPa}^{-1})^{\mathrm{a}}$	${ m L}$	$\mathbf{S}$	${ m L}$	${ m L}$	${f L}$	${ m L}$	$\mathbf{L}$	${ m L}$
$LAI (m^2 m^{-2})$	6	6	6	6	6	6	4	6
$g_{res} \; (\text{mol m}^{-2} \; \text{s}^{-1})$	0.04	0.04	0.02	0.04	0.04	0.04	0.04	0.04
Lower boundary condition <sup>b</sup>	FD	FD	FD	FD	WT	FD	FD	FD
Root distribution <sup>c</sup>	U	U	U	U	U	PW	U	U
Soil type	sand	sand	sand	sandy clay loam	sand	sandy clay loam	sand	sand

<sup>&</sup>lt;sup>a</sup> Two plant hydraulic capacitance: larger (L) and smaller (S)  $C_p$ 's (see Supporting Information).

 $<sup>^{\</sup>rm b}$  Two lower boundary conditions for the soil column: free drainage (FD) and water table (WT) at 2 m depth.

<sup>&</sup>lt;sup>c</sup> Two vertical root distributions: Uniform (U) and power-law (PW) rooting profiles. Note that the power-law reduction function provides a more realistic description for coniferous species (Jackson et al., 1996; Finér et al., 1997; Andersson, 2005).

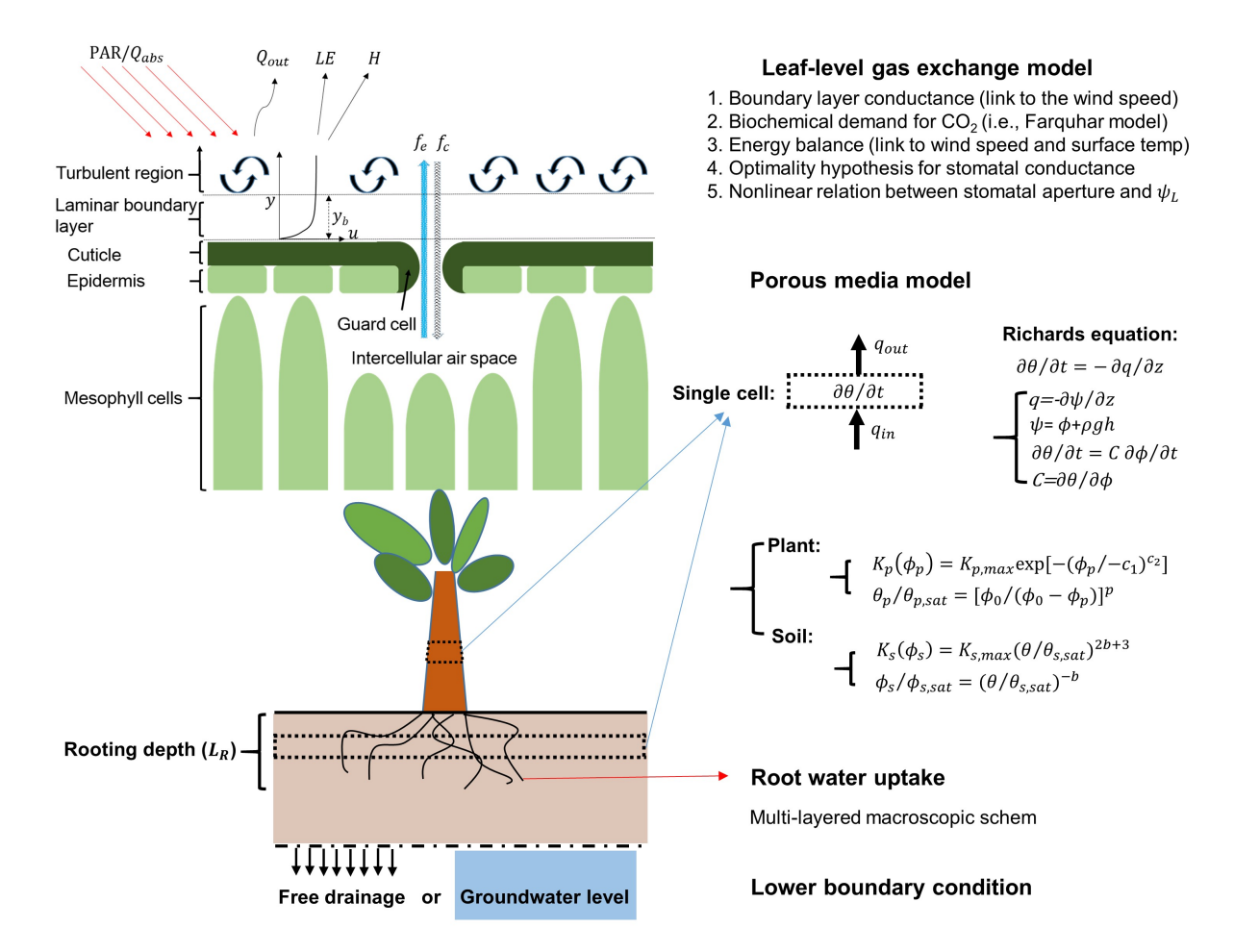


Figure 1: Schematic of the modeling approach describing the water movement through each compartment of the soil-plant-system with a summary of the porous media flow equations used, the lower boundary conditions and the upper boundary conditions represented by the leaf-gas exchange equations.

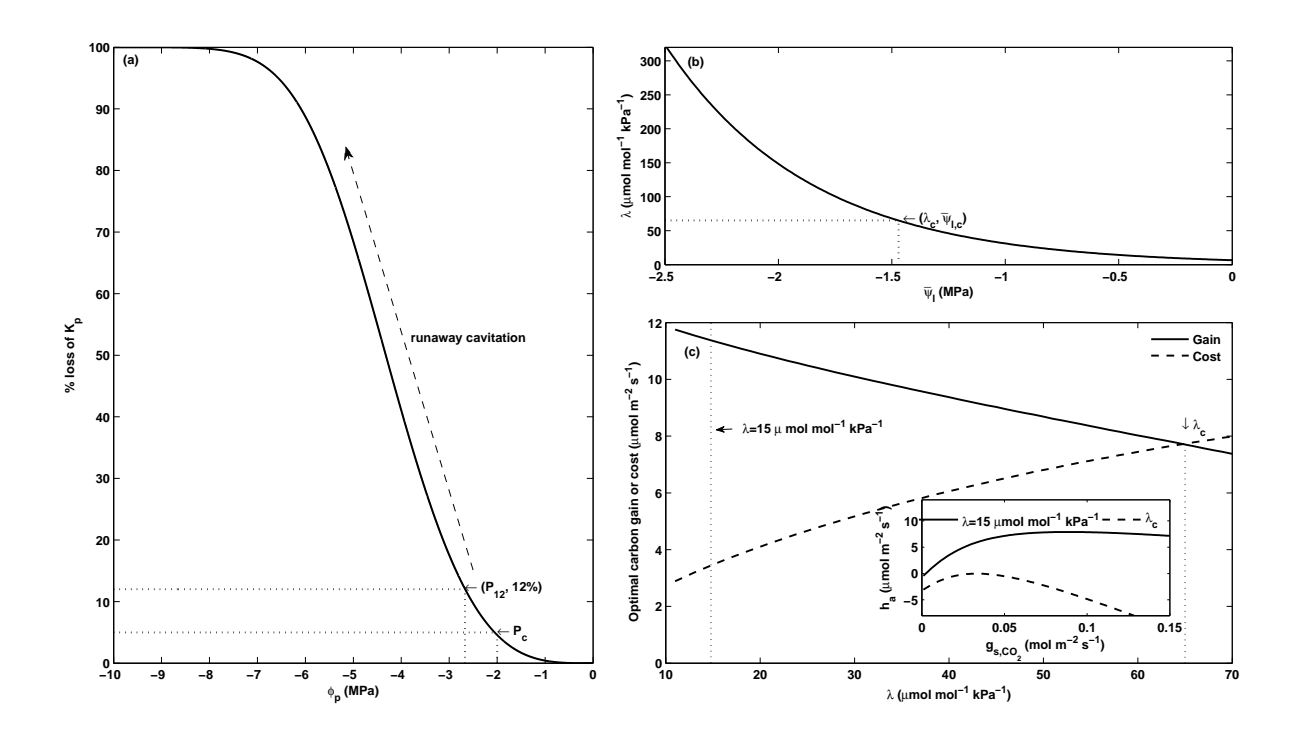


Figure 2: (a) Xylem vulnerability curve with indication of water potentials at 12% loss of  $K_p$   $(P_{12})$  and at complete stomatal closure  $(P_c)$ . (b) The  $\lambda$  values as a function  $\overline{\psi}_l$  using the relation proposed elsewhere (Manzoni et al., 2011). (c) The two components (i.e., carbon gain and water loss in carbon unit) of the optimal 'net' carbon gain  $(h_a)$  as a function of  $\lambda$ . Inset: the 'net' carbon gain  $(h_a)$  as a function of given  $g_{s,CO_2}$  for  $\lambda=15~\mu{\rm mol~mol^{-1}~kPa^{-1}}$  and  $\lambda_c$ . Note that  $\lambda_c$ ,  $\overline{\psi}_{l,c}$  and  $P_c$  are determined at the condition where optimal the 'net' carbon gain is identical to zero (i.e., optimal  $h_a=0$ ).  $\lambda=15~\mu{\rm mol~mol^{-1}~kPa^{-1}}$  is arbitrarily selected to illustrate that  $h_a>0$  when  $\lambda<\lambda_c$ .

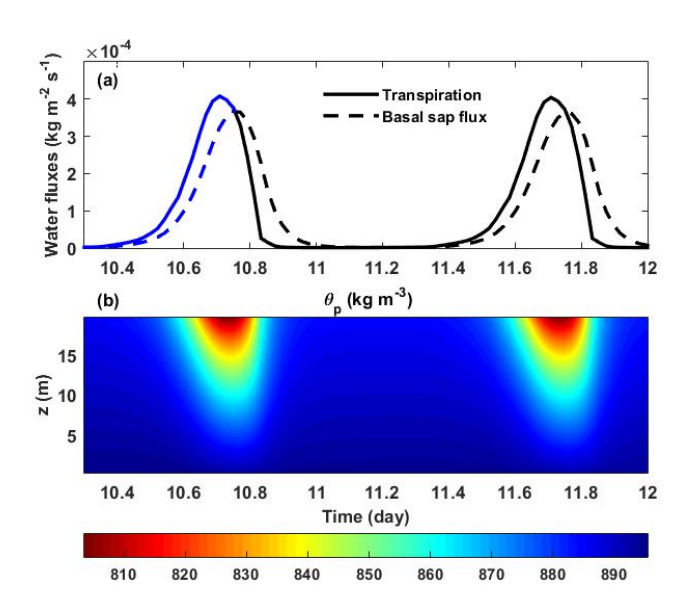


Figure 3: (a) Modeled transpiration rate  $(F_e)$  and basal sap flux  $(q_{p,sb})$  on a per unit ground area basis and (b) modeled profile of plant xylem water content  $(\theta_p)$  with a unit of kg m<sup>-3</sup> for S1 (see Table 1 for model setup). Note that saily PWS usage is determined by the area within the solid and dashed blue lines)

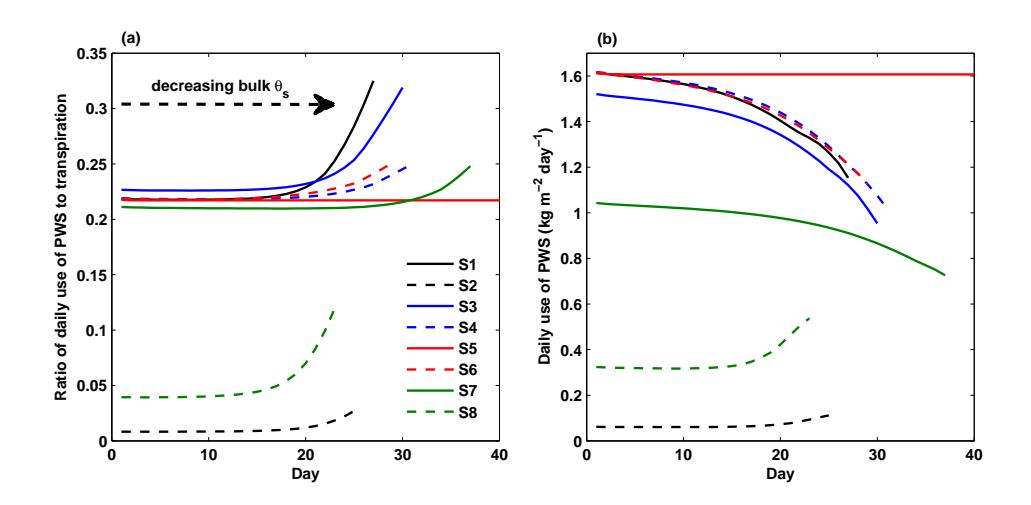


Figure 4: (a) Modeled daily use of plant water storage (PWS) normalized by daily transpiration and (b) modeled daily use of PWS on a per unit ground area basis for the eight scenarios (see Table 1 for the model setup).

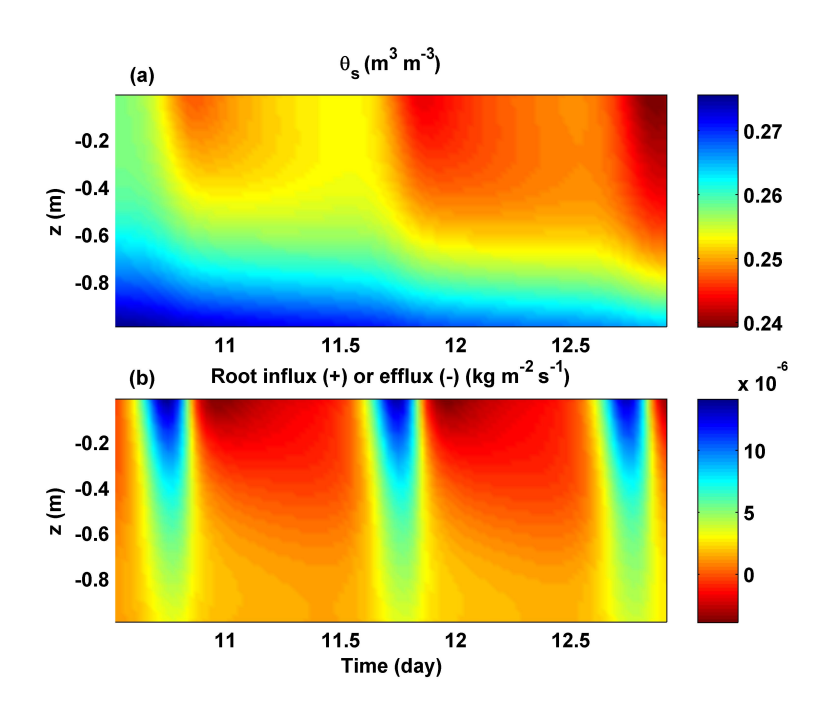


Figure 5: (a) Modeled profiles of soil water content  $(\theta_s)$  and (b) root water influx  $(Q_r^+)$  or efflux  $(Q_r^-)$  on a per unit ground area basis for S6 (see Table 1 for model setup)

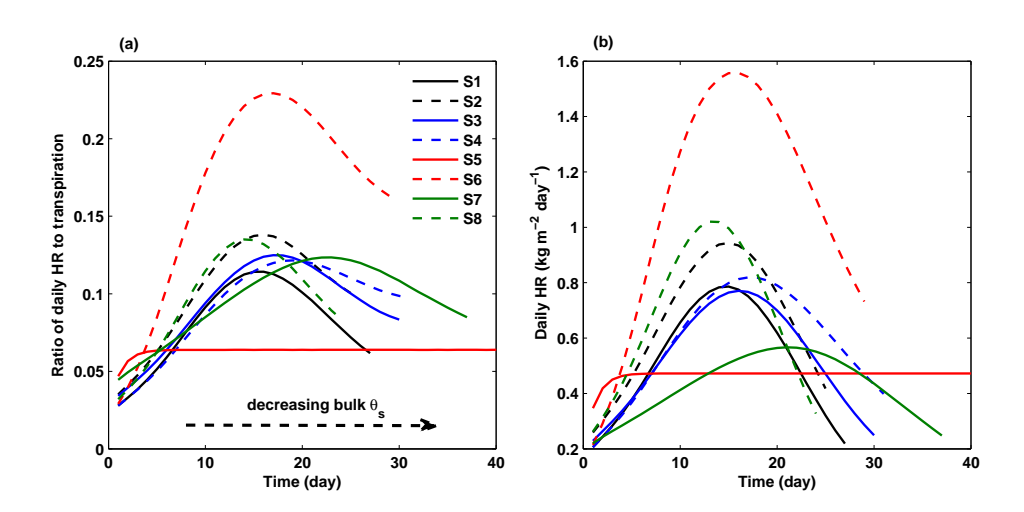


Figure 6: (a) Modeled daily hydraulic redistribution (HR) normalized by daily transpiration and (b) modeled daily HR on a per unit ground area basis for the eight scenarios (see Table 1 for model setup).

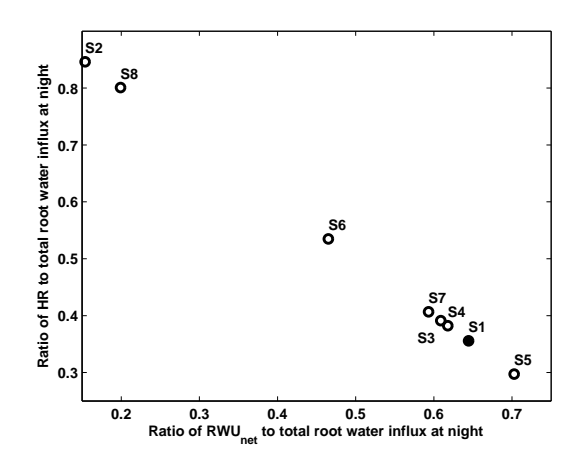


Figure 7: The partitioning between nighttime hydraulic redistribution (HR) and net root water uptake  $(RWU_{net})$  normalized by total root water influx at night over a single dry-down process.

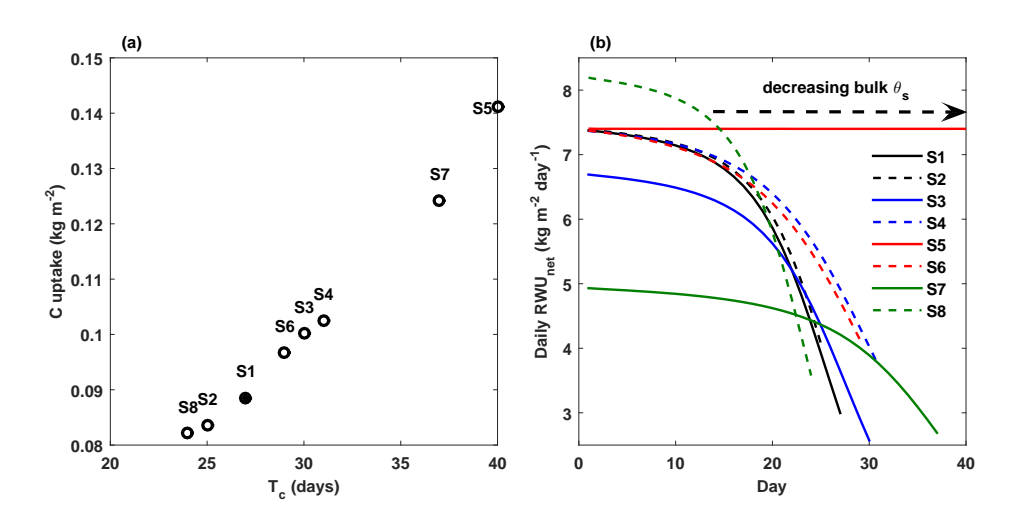


Figure 8: (a) Modeled total carbon uptake  $(C_{uptake})$  on a per unit leaf area basis in relation to the duration before complete stomatal closure  $(T_c)$  for each scenario. (b) Modeled daily net root water uptake  $(RWU_{net})$  on a per unit ground area basis for the eight scenarios (see Table 1 for model setup). Note that  $T_c$  for S5 is indefinite and is terminated at 40 days for reference.

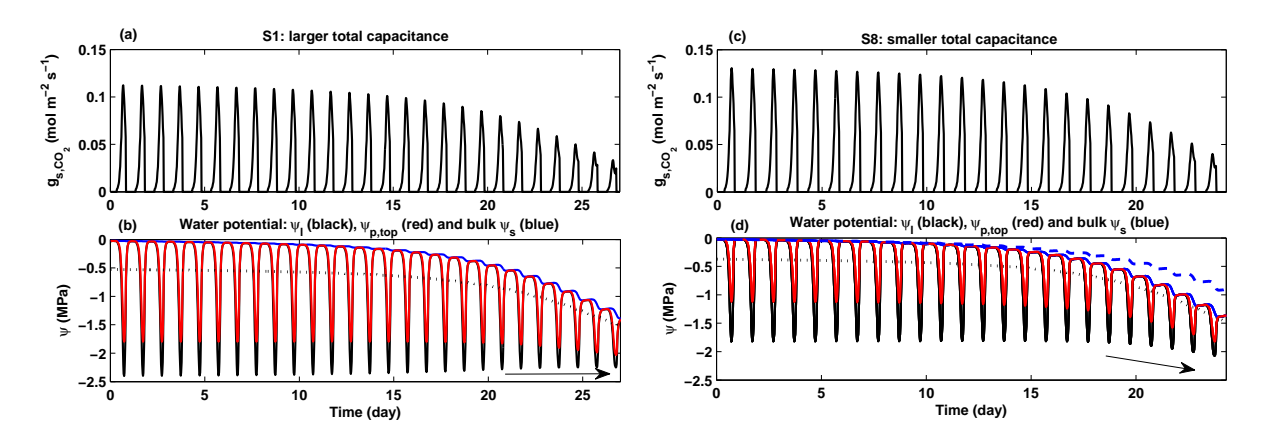


Figure 9: (a) Modeled stomatal conductance  $(g_{s,CO_2})$  and (b) modeled water potential in each compartment for S1. (c) Modeled  $g_{s,CO_2}$  and (b) modeled water potential in each compartment for S8. Note that black solid, black dashed, red solid and blue solid lines are used to represent leaf water potential  $(\psi_l)$ , 24 hours averaged leaf water potential  $(\overline{\psi}_l)$ , distal xylem water potential  $(\psi_{p,top})$  and bulk soil water potential  $(\psi_s)$  across  $L_R$ , respectively. The bulk  $\psi_s$  for S1 (blue dashed line) is also included in Fig. 9d for reference. The  $T_c$ 's for S1 and S8 are respectively 27 and 23 days (i.e., x-axis range for each scenario).

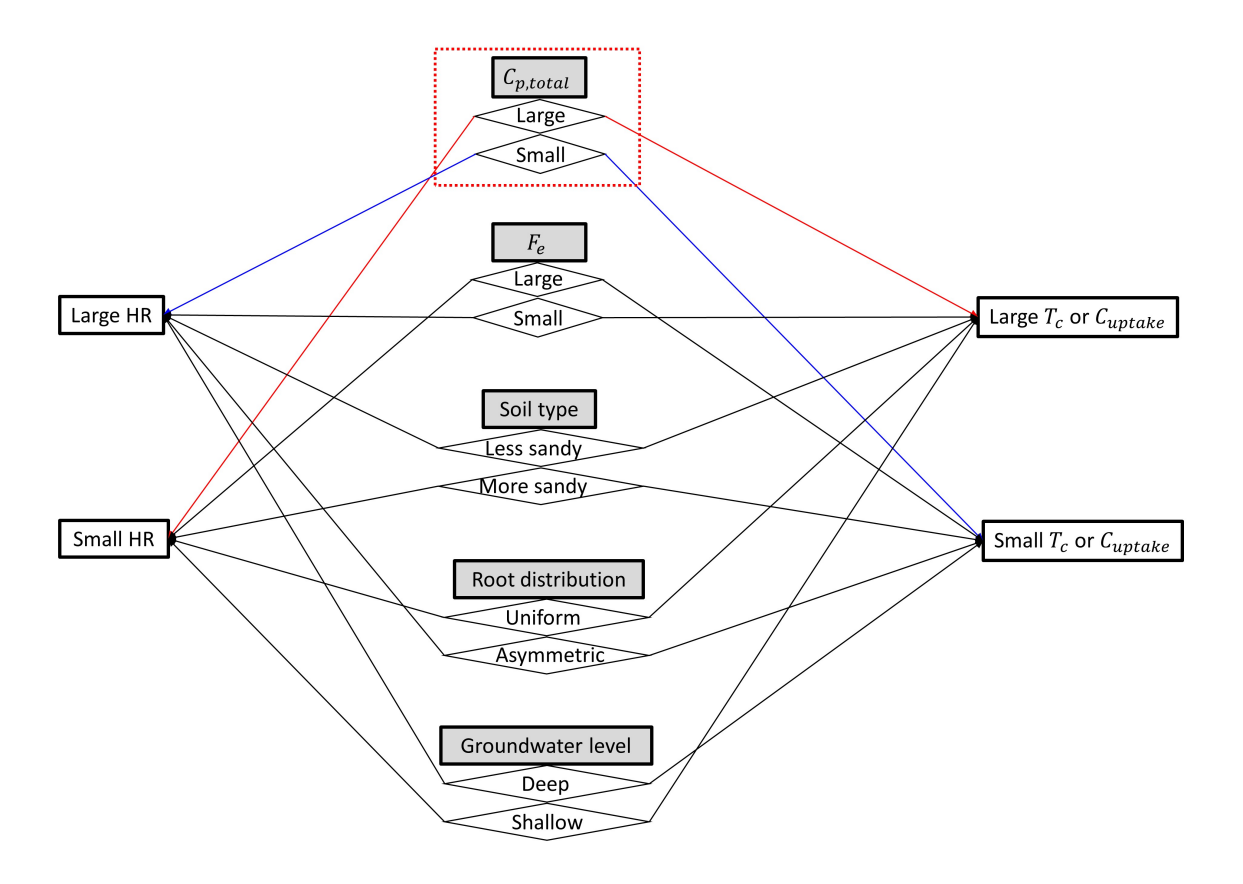


Figure 10: A summary of how exogenous and endogenous factors (i.e., the eight scenarios) impact modeled hydraulic redistribution (HR), duration before complete stomatal closure  $(T_c)$  and total carbon uptake  $(C_{uptake})$  during a dry-down period. Note that all the factors explored here have the same positive or negative effects on HR and  $T_c$  (or  $C_{uptake}$ ) except for  $C_{p,total}$ . Thus, the blue and red lines are used to indicate the opposite trends imposed by  $C_{p,total}$  that is enclosed by the dotted box for clarity.

#### References

- Andersson, F., 2005. Coniferous forests. volume 6. Elsevier, Amsterdam.
- Aumann, C., Ford, E., 2002. Modeling tree water flow as an unsaturated flow through a porous medium. Journal of theoretical biology 219, 415–429.
- Ball, J.T., Woodrow, I.E., Berry, J.A., 1987. A model predicting stomatal conductance and its contribution to the control of photosynthesis under different environmental conditions, in:

  Progress in photosynthesis research. Springer, pp. 221–224.
- Bohrer, G., Mourad, H., Laursen, T., Drewry, D., Avissar, R., Poggi, D., Oren, R., Katul, G., 2005. Finite element tree crown hydrodynamics model (FETCH) using porous media flow within branching elements: A new representation of tree hydrodynamics. Water Resources Research 41.
- Bond, B.J., Kavanagh, K.L., 1999. Stomatal behavior of four woody species in relation to leafspecific hydraulic conductance and threshold water potential. Tree Physiology 19, 503–510.
- Bonetti, S., Manoli, G., Domec, J.C., Putti, M., Marani, M., Katul, G., 2015. The influence of water table depth and the free atmospheric state on convective rainfall predisposition. Water Resources Research 51, 2283–2297.
- Brodribb, T., Cochard, H., 2009. Hydraulic failure defines the recovery and point of death in water-stressed conifers. Plant physiology 149, 575–584.
- Brough, D., Jones, H., Grace, J., 1986. Diurnal changes in water content of the stems of apple trees, as influenced by irrigation. Plant, Cell and Environment 9, 1–7.
- Burgess, S.S., Pate, J.S., Adams, M.A., Dawson, T.E., 2000. Seasonal water acquisition and
   redistribution in the australian woody phreatophyte, *Banksia prionotes*. Annals of Botany
   85, 215–224.
- Caird, M.A., Richards, J.H., Donovan, L.A., 2007. Nighttime stomatal conductance and transpiration in C<sub>3</sub> and C<sub>4</sub> plants. Plant Physiology 143, 4–10.
- Campbell, G.S., Norman, J., 1998. An introduction to environmental biophysics. Springer, New York.
- Chuang, Y., Oren, R., Bertozzi, A., Phillips, N., Katul, G., 2006. The porous media model for the hydraulic system of a conifer tree: Linking sap flux data to transpiration rate. Ecological Modelling 191, 447–468.
- Clapp, R., Hornberger, G., 1978. Empirical equations for some soil hydraulic properties. Water Resources Research 14, 601–604.
- Cowan, I., Farquhar, G., 1977. Stomatal function in relation to leaf metabolism and environment,
   in: Symposia of the Society for Experimental Biology, pp. 471–505.
- Cruiziat, P., Cochard, H., Améglio, T., 2002. Hydraulic architecture of trees: main concepts and results. Annals of forest science 59, 723–752.
- Dawson, T.E., 1993. Hydraulic lift and water use by plants: implications for water balance, performance and plant-plant interactions. Oecologia 95, 565–574.

- Dawson, T.E., Burgess, S.S.O., Tu, K.P., Oliveira, R.S., Santiago, L.S., Fisher, J.B., Simonin,
- K.A., Ambrose, A.R., 2007. Nighttime transpiration in woody plants from contrasting ecosys-
- tems. Tree Physiology 27, 561–575.
- Domec, J., Gartner, B., 2001. Cavitation and water storage capacity in bole xylem segments of mature and young Douglas-fir trees. Trees 15, 204–214.
- Domec, J., King, J.S., Noormets, A., Treasure, E., Gavazzi, M., Sun, G., McNulty, S., 2010.
- 538 Hydraulic redistribution of soil water by roots affects wholestand evapotranspiration and net
- ecosystem carbon exchange. New Phytologist 187, 171–183.
- Dye, P., Soko, S., Poulter, A., 1996. Evaluation of the heat pulse velocity method for measuring
   sap flow in *Pinus patula*. Journal of experimental botany 47, 975–981.
- Edwards, W., Jarvis, P., Landsberg, J., Talbot, H., 1986. A dynamic model for studying flow
   of water in single trees. Tree Physiology 1, 309–324.
- Emerman, S.H., Dawson, T.E., 1996. Hydraulic lift and its influence on the water content of the rhizosphere: an example from sugar maple, *Acer saccharum*. Oecologia 108, 273–278.
- Farquhar, G.D., von Caemmerer, S., Berry, J.A., 1980. A biochemical model of photosynthetic CO<sub>2</sub> assimilation in leaves of C<sub>3</sub> species. Planta 149, 78–90.
- Finér, L., Messier, C., De Grandpré, L., 1997. Fine-root dynamics in mixed boreal conifer broad-leafed forest stands at different successional stages after fire. Canadian Journal of
   Forest Research 27, 304–314.
- Früh, T., Kurth, W., 1999. The hydraulic system of trees: theoretical framework and numerical simulation. Journal of theoretical Biology 201, 251–270.
- Goldstein, G., Andrade, J., Meinzer, F., Holbrook, N., Cavelier, J., Jackson, P., Celis, A., 1998.

  Stem water storage and diurnal patterns of water use in tropical forest canopy trees. Plant,
  Cell and Environment 21, 397–406.
- Granier, A., 1987. Evaluation of transpiration in a Douglas-fir stand by means of sap flow measurements. Tree physiology 3, 309–320.
- Hentschel, R., Bittner, S., Janott, M., Biernath, C., Holst, J., Ferrio, J.P., Gessler, A., Priesack,
   E., 2013. Simulation of stand transpiration based on a xylem water flow model for individual
   trees. Agricultural and Forest Meteorology 182, 31–42.
- Howard, A.R., Van Iersel, M.W., Richards, J.H., Donovan, L.A., 2009. Nighttime transpiration can decrease hydraulic redistribution. Plant, Cell and Environment 32, 1060–1070.
- Huang, C.W., Chu, C.R., Hsieh, C.I., Palmroth, S., Katul, G.G., 2015. Wind-induced leaf transpiration. Advances in Water Resources doi:doi:10.1016/j.advwatres.2015.10.009.
- Hultine, K., Williams, D., Burgess, S., Keefer, T., 2003. Contrasting patterns of hydraulic
   redistribution in three desert phreatophytes. Oecologia 135, 167–175.
- Jackson, R., Canadell, J., Ehleringer, J., Mooney, H., Sala, O., Schulze, E., 1996. A global analysis of root distributions for terrestrial biomes. Oecologia 108, 389–411.
- Kavanagh, K., Bond, B., Aitken, S., Gartner, B., Knowe, S., 1999. Shoot and root vulnerability to xylem cavitation in four populations of Douglas-fir seedlings. Tree Physiology 19, 31–37.

- Konrad, W., Roth-Nebelsick, A., 2003. The dynamics of gas bubbles in conduits of vascular plants and implications for embolism repair. Journal of Theoretical Biology 224, 43–61.
- Kumagai, T., 2001. Modeling water transportation and storage in sapwood-model development and validation. Agricultural and Forest Meteorology 109, 105–115.
- Lafolie, F., Bruckler, L., Tardieu, F., 1991. Modeling root water potential and soil-root water transport: I. Model presentation. Soil Science Society of America Journal 55, 1203–1212.
- Leuning, R., 1995. A critical appraisal of a combined stomatal-photosynthesis model for C<sub>3</sub> plants. Plant, Cell and Environment 18, 339–355.
- Loustau, D., Berbigier, P., Roumagnac, P., Arruda-Pacheco, C., David, J., Ferreira, M., Pereira,
   J., Tavares, R., 1996. Transpiration of a 64-year-old maritime pine stand in portugal. Oecologia
   107, 33-42.
- Maherali, H., DeLucia, E., 2001. Influence of climate-driven shifts in biomass allocation on water transport and storage in ponderosa pine. Oecologia 129, 481–491.
- Manoli, G., Bonetti, S., Domec, J.C., Putti, M., Katul, G., Marani, M., 2014. Tree root systems competing for soil moisture in a 3D soil-plant model. Advances in Water Resources 66, 32–42.
- Manzoni, S., Katul, G., Porporato, A., 2014. A dynamical system perspective on plant hydraulic
   failure. Water Resources Research 50, 5170–5183.
- Manzoni, S., Vico, G., Katul, G., Fay, P.A., Polley, W., Palmroth, S., Porporato, A., 2011.
  Optimizing stomatal conductance for maximum carbon gain under water stress: a metaanalysis across plant functional types and climates. Functional Ecology 25, 456–467.
- Manzoni, S., Vico, G., Katul, G., Palmroth, S., Jackson, R.B., Porporato, A., 2013a. Hydraulic
   limits on maximum plant transpiration and the emergence of the safety-efficiency trade-off.
   New Phytologist 198, 169–178.
- Manzoni, S., Vico, G., Palmroth, S., Porporato, A., Katul, G., 2013b. Optimization of stomatal
   conductance for maximum carbon gain under dynamic soil moisture. Advances in Water
   Resources 62, 90–105.
- Manzoni, S., Vico, G., Porporato, A., Katul, G., 2013c. Biological constraints on water transport
   in the soil-plant-atmosphere system. Advances in Water Resources 51, 292–304.
- McDowell, N., Pockman, W., Allen, C., Breshears, D., Cobb, N., Kolb, T., Plaut, J., Sperry, J., West, A., Williams, D., 2008. Mechanisms of plant survival and mortality during drought: why do some plants survive while others succumb to drought? New phytologist 178, 719–739.
- Meinzer, F., Brooks, J., Bucci, S., Goldstein, G., Scholz, F., Warren, J., 2004. Converging
   patterns of uptake and hydraulic redistribution of soil water in contrasting woody vegetation
   types. Tree Physiology 24, 919–928.
- Neumann, R., Cardon, Z., 2012. The magnitude of hydraulic redistribution by plant roots: a review and synthesis of empirical and modeling studies. New Phytologist 194, 337–352.
- Novick, K.A., Oren, R., Stoy, P.C., Siqueira, M.B.S., Katul, G.G., 2009. Nocturnal evapotranspiration in eddy-covariance records from three co-located ecosystems in the Southeastern U.S.: Implications for annual fluxes. Agricultural and Forest Meteorology 149, 1491–1504.

- Parolari, A.J., Katul, G.G., Porporato, A., 2014. An ecohydrological perspective on droughtinduced forest mortality. Journal of Geophysical Research: Biogeosciences 119, 965–981.
- Phillips, N., Ryan, M., Bond, B., McDowell, N., Hinckley, T., Čermák, J., 2003. Reliance on
   stored water increases with tree size in three species in the Pacific Northwest. Tree Physiology
   23, 237–245.
- Phillips, N.G., Oren, R., Licata, J., Linder, S., 2004. Time series diagnosis of tree hydraulic characteristics. Tree Physiology 24, 879–890.
- Prieto, I., Armas, C., Pugnaire, F., 2012. Water release through plant roots: new insights into its consequences at the plant and ecosystem level. New Phytologist 193, 830–841.
- Prieto, I., Kikvidze, Z., Pugnaire, F., 2010. Hydraulic lift: soil processes and transpiration in the mediterranean leguminous shrub *Retama sphaerocarpa* (L.) boiss. Plant and Soil 329, 447–456.
- Scholz, F., Bucci, S., Goldstein, G., Moreira, M., Meinzer, F., Domec, J.C., Villalobos-Vega, R.,
   Franco, A., Miralles-Wilhelm, F., 2008. Biophysical and life-history determinants of hydraulic
   lift in Neotropical savanna trees. Functional Ecology 22, 773–786.
- Schulze, E.D., Čermák, J., Matyssek, R., Penka, M., Zimmermann, R., Vasícek, F., Gries, W.,
   Kučera, J., 1985. Canopy transpiration and water fluxes in the xylem of the trunk of larix
   and picea treesa comparison of xylem flow, porometer and cuvette measurements. Oecologia
   66, 475–483.
- Schymanski, S., Sivapalan, M., Roderick, M., Beringer, J., Hutley, L., 2008. An optimality-based
   model of the coupled soil moisture and root dynamics. Hydrology and Earth System Sciences
   Discussions 12, 913–932.
- Siqueira, M., Katul, G., Porporato, A., 2008. Onset of water stress, hysteresis in plant conductance, and hydraulic lift: scaling soil water dynamics from millimeters to meters. Water
   Resources Research 44.
- Sparks, J., Black, R., 1999. Regulation of water loss in populations of *Populus trichocarpa*: the role of stomatal control in preventing xylem cavitation. Tree Physiology 19, 453–459.
- Sperry, J., Love, D., 2015. What plant hydraulics can tell us about responses to climate-change droughts. New Phytologist 207, 14–27.
- Sperry, J., Tyree, M., 1990. Water-stress-induced xylem embolism in three species of conifers.
  Plant, Cell and Environment 13, 427–436.
- Stratton, L., Goldstein, G., Meinzer, F., 2000. Stem water storage capacity and efficiency of water transport: their functional significance in a hawaiian dry forest. Plant, Cell and Environment 23, 99–106.
- Taneda, H., Tateno, M., 2011. Leaf-lamina conductance contributes to an equal distribution of
   water delivery in current-year shoots of kudzu-vine shoot, pueraria lobata. Tree physiology
   31, 782–794.
- Tuzet, A., Perrier, A., Leuning, R., 2003. A coupled model of stomatal conductance, photosynthesis and transpiration. Plant, Cell and Environment 26, 1097–1116.
- Tyree, M., 1988. A dynamic model for water flow in a single tree: evidence that models must account for hydraulic architecture. Tree Physiology 4, 195–217.

- Tyree, M., Davis, S., Cochard, H., 1994. Biophysical perspectives of xylem evolution: is there a tradeoff of hydraulic efficiency for vulnerability to dysfunction? IAWA journal 15, 335–360.
- Tyree, M., Ewers, F., 1991. The hydraulic architecture of trees and other woody plants. New Phytologist 119, 345–360.
- Tyree, M., Sperry, J., 1989. Vulnerability of xylem to cavitation and embolism. Annual Review
   of Plant Biology 40, 19–36.
- Tyree, M., Yang, S., 1990. Water-storage capacity of *Thuja*, *Tsuga* and *Acer* stems measured by dehydration isotherms. Planta 182, 420–426.
- Tyree, M., Zimmermann, M., 2002. Xylem structure and the ascent of sap. Springer.
- Vogel, T., Dohnal, M., Dusek, J., Votrubova, J., Tesar, M., 2013. Macroscopic modeling of plant
   water uptake in a forest stand involving root-mediated soil water redistribution. Vadose Zone
   Journal 12.
- Volpe, V., Marani, M., Albertson, J.D., Katul, G.G., 2013. Root controls on water redistribution and carbon uptake in the soil-plant system under current and future climate. Advances in Water Resources 60, 110–120.
- Wang, X., Tang, C., Guppy, C., Sale, P.W.G., 2009. The role of hydraulic lift and subsoil P placement in P uptake of cotton (*Gossypium hirsutum* L.). Plant and Soil 325, 263–275.
- Waring, R., Running, S., 1978. Sapwood water storage: its contribution to transpiration and effect upon water conductance through the stems of old-growth Douglas-fir. Plant, Cell and Environment 1, 131–140.
- Waring, R., Whitehead, D., Jarvis, P., 1979. The contribution of stored water to transpiration in Scots pine. Plant, Cell and Environment 2, 309–317.
- Warren, J., Meinzer, F., Brooks, J., Domec, J., 2005. Vertical stratification of soil water storage and release dynamics in Pacific Northwest coniferous forests. Agricultural and Forest
   Meteorology 130, 39–58.
- Yoder, C.K., Nowak, R.S., 1999. Hydraulic lift among native plant species in the Mojave Desert.
  Plant and Soil 215, 93–102.
- Zang, D., Beadle, C., White, D., 1996. Variation of sapflow velocity in *Eucalyptus globulus* with position in sapwood and use of a correction coefficient. Tree Physiology 16, 697–703.
- <sup>660</sup> Zimmermann, M.H., 1983. Xylem structure and the ascent of sap. Springer.